RUVBL1 and RUVBL2 as novel druggable DNA Damage Response regulators in the N-Myc regulatory network in neuroblastoma

Jimmy Van den Eynden (jimmy.vandeneynden@ugent.be)
Ghent University https://orcid.org/0000-0003-0002-5614
Joachim Siaw
Ghent University
Arne Claeys
Ghent University
Wei-Yun Lai
University of Gothenburg
Marcus Borenäs
University of Gothenburg
Elien Hilgert
Ghent University
Sarah-Lee Bekaert
Ghent University
Franki Speleman
University Hospital Ghent https://orcid.org/0000-0002-6628-8559
Kaat Durinck
Ghent University
Bengt Hallberg
University of Gothenburg
Ruth H Palmer
University of Gothenburg

Article

Keywords: Neuroblastoma, RUVBL1, RUVBL2, MYCN, ATR, CB-6644

Posted Date: November 20th, 2023

DOI: https://doi.org/10.21203/rs.3.rs-3206227/v1

Additional Declarations: (Not answered)

Abstract

High-risk neuroblastoma (NB) accounts for about 50% of all cases. These tumours are characterized by *MYCN* amplification and high *MYC* gene expression and patients have a high relapse rate despite intensive therapies, hence the need for safer and more effective drugs. Strategies to develop inhibitors that directly target the MYC proteins have been elusive.

Based on in silico molecular signature score and network analyses, we identified RUVBL2 as a key interactor of MYC. Kaplan-Meier survival and multivariate Cox regression analyses using public NB datasets demonstrated that expression of RUVBL2 and its interaction partner RUVBL1 are strong and independent predictors for both overall and event-free survival in NB patients. Using different types of NB cell lines, we experimentally demonstrated that transient knockdown of RUVBL1/2 or pharmacological inhibition using CB-6644 resulted in cell cycle arrest, cell growth arrest and a DNA Damage Response (DDR) through regulation of ATR and ATM. Additionally we confirmed that RUVBL1/2 transcriptionally regulate MYCN and MYC.

Our work demonstrates that RUVBL1 and RUVBL2 are novel regulators of the DDR with therapeutic and independent prognostic potential in high-risk NB.

Introduction

Neuroblastoma (NB) is the most common cancer of infancy. It arises from neural crest derived immature sympathoblasts and occurs along the sympathetic chain ganglia and in the adrenal gland.[1,2] Despite the improvement in the overall survival (OS) and event-free survival (EFS) of NB patients over the years, more than 50% of high-risk patients relapse and succumb to the disease in spite of intensive multimodal therapies, including both standard and high-dose chemotherapy.[3–5] Additionally, severe life-threatening toxicities occur in many of the high-risk patients during and after treatment with cytotoxic chemotherapy and radiotherapy.[3,6] Hence, novel, safer and more effective drugs are urgently needed to treat high-risk NB. Tumour stage, *MYCN* amplification status and age at diagnosis are the most commonly used prognostic biomarkers in risk stratification of children with NB.[5,7,8] Other studies have reported on telomere maintenance mechanism and its emerging role as a strong prognostic biomarker associated with high-risk NB.[9–11] The relatively high relapse rate in high-risk NB patients continues to spur strategies for identification of novel molecular targets and development of effective therapies against this malignancy.

NB is characterised by recurrent patterns of distinct segmental chromosomal aberrations including chromosome 11q deletion which results in loss of tumour suppressors like *SHANK2* and *DLG2*, 1p deletion, 17q gain, 2p gain and *MYCN* amplification, while the mutational burden is low.[12–15] The rarity of druggable recurrent mutations is a major bottleneck to the development of effective targeted therapies against high-risk NB. *MYCN* amplification and high *MYC* expression are thought to be associated with majority of high-risk NB, and consistently predict poor prognosis.[16–19] Developing inhibitors that directly

target MYC(N) proteins has proven challenging, except for Omomyc, a distinctive peptide created approximately two decades ago again C-Myc.[20,21] Omomyc forms dimers with C-Myc, disrupting its DNA binding abilities, and has demonstrated promising results in a recently concluded phase I clinical trial.[21,22] Indirect approaches to target MYCs include targeting epigenetic regulators of *MYC(N)* expression or their mRNA and protein stability, have also produced limited results,[23–25] hence, novel inhibitors or strategies are urgently needed.

In this study, *RUVBL2* (*RuvB like AAA ATPase 2;* also known as *Reptin*, *TIP48*, *TIP49b* or *Rvb2*) was detected as an important interactor with *MYC*. *RUVBL2* and the related *RUVBL1* (also known as *Pontin*, *TIP49*, *TIP49a* or *Rvb1*) are members of the AAA+ (*ATPase* associated with diverse cellular activities)-family of ATPases. RUVBL2 usually forms heterohexamers or heterododecamers with RUVBL1 and largely overlap at active gene promoters.[26,27] They have functional roles in epigenetic regulation of gene expression, cell proliferation, DNA repair, regulation of telomerase activity, senescence and transcriptional co-activation.[26,28–32] RUVBL1/2 have been implicated in cancer and their prospects as potential therapeutic targets in cancer led to the recent identification and development of inhibitors, such as CB-6644.[33–36]

Here, we identified *RUVBL1/2* as independent prognostic biomarkers in NB, after correcting for *bonafide* NB biomarkers. We showed that *RUVBL1/2* are novel dependency factors, and their knockdown with siRNA or inhibition with CB-6644 blocked *MYCN* and *MYC* expression and caused elevated DNA damage response, cell cycle arrest and apoptosis in several independent NB cell lines. In line with this finding, combined RUVBL1/2 and ATR inhibition potently induced DNA damage and apoptotic cell death of NB cell lines. Altogether, we show *RUVBL1/2* are regulators of DNA damage response (DDR), promising new biomarkers and putative therapeutic targets in high-risk NB.

Methods

Data download and processing

Human NB RNA-seq and related clinical data generated by the Therapeutically Applicable Research to Generate Effective Treatments (TARGET) initiative (phs000467) (NB-TARGET) were downloaded from the Genomic Data Commons (GDC) portal (https://portal.gdc.cancer.gov/projects/TARGET-NBL; 155 primary NB tumour samples).[37] RNA-seq data from other primary tumour NB samples referred to as NB-SEQC (GSE62564) was downloaded from Gene Expression Omnibus.[38,39] NB-Cangelosi dataset (786 primary tumours),[40] is a dataset compiled by integrating other NB data cohorts including parts of NB-SEQC. Therefore, we filtered out all samples which are part of the NB-SEQC dataset to obtain two non-overlapping data cohorts: NB-SEQC (n = 498) and filtered NB-Cangelosi (n = 419). Gene expression data for NB cell lines were downloaded from DepMap (https://depmap.org/portal; CCLE project, 32 NB cell lines).

Microarray data for mice model of *Th-MYCN*-driven NB were obtained from ArrayExpress (accession number E-MTAB-3247).[41] Background correction and quantile normalization of these data were performed using the *Limma* v.3.50.3 *R* package.[42] Gene expression of *Ruvbl1*, and *Ruvbl2* was evaluated at 1, 2, and 6 weeks. Genes differentially expressed between *Th-MYCN*$^{+/+}$ and wild-type mice at week 6 were determined using *Limma* moderated t-statistics to determine significance in gene expression changes.

Gene effect scores (dependency scores) of 34 NB cell lines, derived from CRISPR knockout screens and published by Broad's Achilles and Sanger's SCORE projects, were downloaded from DepMap,[43] (https://depmap.org/portal/download/all/). Negative gene effect scores imply cell growth inhibition and/or death following gene knockout. Non-essential genes have a normalised median score of 0 and predefined common essentials have a median score of -1. Essential genes (n = 1910) were derived from DepMap.

Signature score and network analysis

Transcriptomic count data (NB-TARGET) were first normalized to FPKM after which signature scores were calculated using the *R* package *singscore v.1.10.0*,[44] using the Hallmark gene set downloaded from Molecular Signatures Database v7.5.1,[45] (https://www.gsea-msigdb.org/gsea/msigdb/). Network analyses were performed in *Cytoscape* (v3.9.1),[46] using the *STRING* module (https://string-db.org/). Embedded STRING enrichment analysis was performed to identify enriched KEGG pathways in the network.

Survival analysis

Overall survival (OS) analyses were performed using the *R* packages *Survival* v.3.5-0,[47] and *Survminer* v.0.4.9 and OS curves were plotted by the Kaplan-Meier method. Tumour samples (NB-SEQC and NB-Cangelosi) were stratified (high vs low gene expression) based on median gene (*RUVBL1* or *RUVBL2*) expression. Log-rank tests were performed to assess statistical significance. Multivariate Cox proportional hazards regression model (*R* packages: *Survival* and *Survminer)* was used to evaluate the prognostic values of genes. Tumour stage (stage 4 vs stages 1,2,3), age at diagnosis (> 18 months vs < 18 months) and *MYCN* amplification were used as covariates in the multivariate analysis. A Pearson correlation was calculated between *RUVBL1* and *RUVBL2* expression.

Gene set enrichment analysis and transcription factor predictions

Gene set enrichment analysis (GSEA) was performed using default settings from the R package *fgsea* v.1.20.0,[48] and illustrated using the *clusterprofiler* v.4.2.2 R package.[49] For analysis of RNA-seq data, gene ranking was based on the DEseq2 statistic (Wald statistic) while for analyses of *RUVBL1* or *RUVBL2* tumour gene expression correlation data, gene ranking was based on correlation coefficient. Reactome pathways, Hallmark and transcription factor target gene sets were downloaded from the Molecular

Signatures Database v7.5.1. Only protein-coding transcription factors (TFs) were considered for further analysis.

Antibodies and inhibitors

Primary antibodies against ATR (#13934, RRID:AB_2798347, 1:1000), pATR (#2853, RRID:AB_2290281, 1:1000), ATM (#2873, RRID:AB_2062659, 1:1000), Chk1(#2345, RRID:AB_10693648, 1:1000), pChk1(#2348, RRID:AB_331212 1:1000), β-Actin (#4970, RRID:AB_2223172, 1:10,000), FOXM1 (#20459, RRID:AB_2798842, 1:1000), pFOXM1 (#14655, RRID:AB_2798557, 1:1000), cleaved caspase-3 (#9661, RRID:AB_2341188, 1:1000), phosphor histone H3 (9701, RRID:AB_331535, 1:1000), GAPDH (#5174, RRID:AB_10622025, 1:5000), N-Myc (#9405, RRID:AB_10692664, 1:2000), C-Myc (#18583, RRID:AB_2895543, 1:2000) and PARP (#9542, RRID:AB_2160739, 1:2000) were obtained from Cell Signaling Technology. HRP-conjugated secondary antibody goat anti-rabbit IgG (# 32260, RRID:AB_1965959, 1:5000) were purchased from Thermo Fisher Scientific. RUVBL1/2 inhibitor CB-6644 (# HY-114429) and ATR inhibitor BAY-1895344/ elimusertib (S9864) were purchased from MedChemExpress and Selleck Chemicals respectively.

Cell culture

Cell lines used were CLB-BA, CLB-GE, CLB-GA, NB-1, SK-N-AS, SHSY5Y, SK-N-BE(2). CLB-BA (*MYCN*-amplified), CLB-GE (*MYCN*-amplified) and CLB-GA (*MYCN*-nonamplified) were obtained from The Centre Leon Berard, France under MTA. SK-N-AS (*MYCN*-nonamplified) and SH-SY5Y (*MYCN*-nonamplified) cell lines were purchased from ECACC. Cell lined were cultured in complete media, RPMI 1640 supplemented with 10% foetal bovine serum (FBS) and a mixture of 1% penicillin/streptomycin at 37°C and 5% CO_2.

Mouse tumour-derived NB cell culture and RUVBL1/2 inhibitor treatment

Tumours from two mice with different genetic background, *Alk-F1178S*KI/0;*Th-MYCN*Tg/0,[50] and *Th-MYCN*Tg/0,[51] on a 129X1/SvJ strain (> N10) were harvested and dissociated into single cell suspension. Animal work was conducted following the Gothenburg Animal Ethics Committee approval, Jordbruksverket (1890–2018, 3225–2020). The dissociated cells were cultured in RPMI1640 with 10% FBS and 1% penicillin/streptomycin (Gibco BRL, Life Technologies) and seeded in 96-well plates precoated with 0.4% solution of type I bovine collagen solution (Advanced BioMatrix) for 18 h. Then, cells were treated with increasing concentrations of CB-6644 for 5 d and cell viability was determined by CellTiter-Glo 3D cell viability assay (Promega) according to the manufactures' protocol.

IC_{50} determination, drug combination treatment and other biochemical analysis

Cells were seeded, at cell density between 3000 and 5000 cells/well of 96-well plate, depending on cell type. For IC_{50} determination, cells treated with increasing concentration of CB-6644 and cell viability was assessed after 3 days. To evaluate the effect of CB-6644 on RUVBL1/2 and downstream targets, NB cell lines (CLB-BA, CLB-GA, NB1 and SK-N-AS) were treated with 250 nM CB-6644 for 24, 48 and 72 hrs.

To analyse the effect of CB-6644 (RUVBL1/2 inhibitor) and elimusertib (BAY-1895344; ATR inhibitor) combination treatment on cell proliferation, cells seeded in 96-well plates were treated with either CB-6644 (25, 50 or 100 nM) or elimusertib (5, 10 or 20 nM) or combination of these drugs at constant ratio of 5:1 (CB-6644: elimusertib). Cell confluency/proliferation was monitored live using the IncuCyte® S3 Live Cell Analysis system (Essen BioScience) for 5 days. Rate of cell growth under all conditions were determined using the IncuCyte® S3 software. For biochemical analyses of the combination treatment, cells seeded in 6-well plates were treated with either 100 nM CB-6644 or 20 nM elimusertib or both for 48 hrs. DMSO was used as negative control.

Immunoblotting analyses

Protein lysates were collected by lysing cells in RIPA lysis buffer and protein concentration was measured by BCA assay. Samples were subjected to western blot analyses. Chemiluminescence detection was done using Odyssey Fc Imager (LI-COR). Immunoblots were quantified using Image Studio Lite (v5.2) software.

Synergy calculation

To determine synergy in the combination treatment with CB-6644 and elimusertib, Combination Index (CI) values were determined using the CompuSyn softerware. CI values were calculated according to the Chou and Talalay method,[52] for combinations of different drug concentrations.

Cell cycle analysis

Human NB cell lines SK-N-AS and CLB-GA (6.5 x 10^5 to 1 × 10^6) were seeded in a T-25 flask. After overnight culturing, CB-6644 compound (IC50 (250 nM (SK-N-AS), 120 nM (CLB-GA)) was added, DMSO was used as a control for 48 hrs. Cells were washed once with ice-cold PBS before collection in Phosphate-buffered saline (PBS). During each wash step, cells were centrifuged for 5 minutes at 1200 rpm and supernatant was removed. Cells were washed once in ice-cold PBS before fixation in 70% ethanol for at least 1 hour on ice, then washed once with ice-cold PBS and incubated in PBS with ribonuclease A (RNase A, 250 µg/mL) for 1 hour at 37°C. Propidium iodide (40 µg/mL) was added, and analysis was performed on a BD LSR II flow cytometer using BD FACSDIVATM Software. The flow cytometry results were analysed using FlowJoTM v10.8 Software (BD Life Sciences).

Foci formation assay

Cells (1.0 × 10^5) were seeded in 6-well plates and cultured overnight prior to treated with 250 nM CB-6644 for 14 days. Cells were washed in PBS and fixed with methanol, followed by staining with 0.2% crystal violet, and washed. Plates were then scanned using Toshiba Studio 2505AC.

siRNA-mediated knockdown of RUVBL1/2

NB cells were transfected with Silencer select siRNAs (Life Technologies) against *RUVBL1* [ID # S16369 (siRUVBL1 #1) and S16370 (siRUVBL1 #2)] and *RUVBL2* [ID # S21307 (siRUVBL2 #1) and S21309

(siRUVBL2 #2)] using lipofectamine RNAiMAX transfection reagent (# 13778150, ThermoFisher Scientific). Scrambled siRNA (# S103650325, Qiagen) was used as negative control. Cells were harvested after overnight transfection and seeded (2.5 x 10^3 to 4 x 10^3) in 96-well plates.The remaining cells were seeded in 6-well plates and cultured for 5 days and lysed in RIPA buffer for western blot analysis. The 96-well plates were monitored for cell proliferation using the IncuCyte® S3. Rate of cell growth were determined using the IncuCyte® S3 software.

RNA isolation

MYCN-amplified (CLB-BA) and high *MYC* expressing (SK-N-AS) NB cell lines were treated with 250 nM CB-6644 for 24, 48 and 72 hrs. DMSO was used as negative control. RNA was extracted from the cell pellets using the ReliaPrep™ RNA Miniprep Systems (Promega) and the manufacturers protocol was followed. RNA samples were either used for RNA-seq or quantitative PCR.

RNA-sequencing analysis

RNA isolated from CLB-BA and SK-N-AS cells treated with the RUVBL1/2 inhibitor CB-6644 at 24h, 48h and 72h were subjected to RNA sequencing (Biomarker Technologies, BMK, Germany). RNA-seq paired-end reads (read length 150 base pairs) were aligned to the GRCh38 reference genome using HISAT2.[53] The average alignment efficiency for all samples was 93.4%. Genes were annotated using GENCODE 29 (human) and quantified using HTSeq.[54] Further analysis was performed using only coding genes. Differential gene expression was determined using DESeq2.[55] Only expressed genes, defined as genes with a basemean value higher than 10, were considered for further analysis. Genes were considered differentially expressed if their absolute log2 fold change values were above 1 at FDR-adjusted p values (*Padj*) below 0.05.

Quantitative PCR

RNA samples were subjected to cDNA synthesis using the iScript cDNA synthesis kit (Biorad). Quantitative PCR was performed on StepOnePlus Real-Time PCR Systems using Power SYBR® Green master mix and following primers: *MYCN*: 5'-CTGAGCGATTCAGATGATGAAG-3' and 5'-CCACAGTGACCACGTCGATT-3'; *MYC*: 5'-CAGCTGCTTAGACGCTGGAT-3' and 5'-AGCTAACGTTGAGGGGCATC-3'; *ACTB*: 5'-ATGACCCAGATCATGTTTGAGAC-3' and 5'-CCAGAGGCGTACAGGGATAG-3'.

Data analysis and statistics.

Statistical analyses were performed with R statistical package (v4.0). Statistical tests are indicated in the respective sections and figure captions. Multiple testing corrections were performed using the Benjamini-Hochberg method (Benjamini & Hochberg, 1995).

Results

In silico identification of *RUVBL2* as a key *MYC* interactor.

To identify key genes underlying high-risk NB, we first performed a rank-based Hallmark gene set signature score analysis on publicly available NB primary tumour (TARGET-NBL) and cell line (CCLE project) gene expression data. The highest scores were found for the *MYC-targets-v1* gene set, indicating relative high expression of the involved genes. This gene set, hereafter referred to as the *MYC* signature, showed the highest score in both high-risk NB tumours and cell lines, and also had the second highest score in low-risk NB (Fig. 1a, Figure S1a-b).

We then used a STRING network analysis to screen this *MYC* signature for novel dependency signalling nodes. Several functional modules were identified in this network, including spliceosome, DNA replication, cell cycle, ribosome, proteosome and base excision repair (Fig. 1b), consistent with the role of *MYC(N)* in regulating these pathways in NB and other cancers.[17] *MYC* showed interactions with the cell cycle and spliceosome module (Fig. 1b). Interestingly, *RUVBL2* was identified as a key interactor with *MYC*, and with both the DNA replication and spliceosome modules (Fig. 1b). RUVBL2 plays a role in DNA replication, acts as a coactivator for RNA polymerase II (Pol II) transcriptional activity and is part of multiprotein complex which regulates U5 snRNP, a central component of the spliceosome.[26,56,57] RUVBL2 and the related RUVBL1 are members of the AAA+ (ATPase associated with diverse cellular activities)-family of ATPases. RUVBL1 and RUVBL2 stabilize each other and form ring-shaped hetero-hexameric complex that display a synergistic ATPase activity.[27] The cellular/molecular role(s) of RUVBL1/2 in NB have not previously been investigated.

RUVBL1/2 expression is a prognostic marker of high-risk NB.

We next assessed *RUVBL1/2* expression levels as potential biomarkers for high-risk NB. As expected, *RUVBL1*/2 expression was higher in *MYCN*-amplified tumours as compared to non-amplified tumours (P = 2.2e-16; unpaired, two-sided t-test, Fig. 1c, Figure S1c). Furthermore, the highest expression levels were found for stage 4 tumours (P = 2.2e-16, when comparing to stage 1 tumours; Figure S1d) and in patients older than 18 months at diagnosis (P = 2.2e-16 and P = 1.2e-12, Figure S1e). To further explore high *RUVBL1/2* expression as unfavourable prognostic markers in NB, we determined the association of *RUVBL1/2* expression levels with patient outcome. Patients with higher-than-median *RUVBL1/2* expression had poor overall survival (P < 0.0001; log-rank test; Fig. 1d, Figure S1f) and poor event-free survival (P < 0.0001: Figure S1g-h) in a Kaplan-Meier analysis, consistent with the correlation of high *RUVBL1/2* mRNA levels with unfavourable prognostic markers.

Interestingly, when considering *bonafide* prognostic NB biomarkers as covariates (i.e., tumour stage, age at diagnosis and *MYCN* amplification),[7] *RUVBL1* and *RUVBL2* were identified as independent prognostic biomarkers in a multivariate Cox proportional hazards regression (*RUVBL1*: hazard ratio [HR] = 3.4, P = 5.9e-4; *RUVBL2*: HR = 2.8, P = 1.2e-3; Fig. 1e) and Kaplan-Meier (Figure S1i) analyses in the NB-SEQC cohort. These HRs are notably close in comparison to *MYCN*-amplification, which is widely recognized as one of the most powerful indicators of unfavourable prognosis in NB (HR = 2.6, P = 6.0e-05; HR = 2.5, P =

2.4e-05). Interestingly, when repeating this analysis for all other coding genes, *RUVBL1* and *RUVBL2* had HRs that were higher than 96% and 99% of all coding genes, respectively (Fig. 1f, Table S1). Similar results were obtained for the independent NB-Cangelosi primary tumour cohort (Figure S1j-k, Table S1). Altogether, these results suggest *RUVBL1/2* are independent prognostic markers for high-risk NB.

NB cells depend on *RUVBL1/2* for survival.

To find support for functional roles of *RUVBL1/2* in NB, we analysed publicly available gene dependency scores of 34 NB cell lines, with negative scores indicating gene dependency. Interestingly, both *RUVBL1* (median score = -1.83) *and RUVBL2* (median score = -1.75) had significantly lower scores than a previously identified set of 1910 essential genes,[43] (median score = -1.00; $P < 0.0001$; unpaired Wilcox test; Fig. 2a).

We confirmed *RUVBL1/2* expression in NB cell lines and found that *RUVBL1* and *RUVBL2* expression were strongly correlated, both in cell lines (Pearson's $R = 0.78$; Figure S2a-b) and in primary NB tumour cohorts ($R = 0.71$ [NB-SEQC] and $R = 0.82$ [NB-Cangelosi]; Figure S2c-d), indicating the two genes might be coregulated. During early tumour development in *Th-MYCN* mice, both genes are increasingly expressed from hyperplastic lesions towards full blown tumours (Figure S2e).

To evaluate the effect of RUVBL1/2 downregulation, we carried out transient knockdown using two independent pairs of small interfering RNAs (siRNAs) in a high-risk NB-derived cell line, SK-N-AS. Each specific siRNA efficiently knocked down its target, RUVBL1 or RUVBL2 and, remarkably, knockdown of RUVBL1 also resulted in downregulation of RUVBL2 protein, and vice versa (Fig. 2b). This result is consistent with earlier findings showing that RUVBL1 and RUVBL2 are coregulated through a post-translational mechanism.[58] Transient siRNA-mediated downregulation of either RUVBL1 or RUVBL2 or both together, led to abrogation of proliferation of three independent NB cell lines: *MYCN*-amplified CLB-BA and NB1 cells, and *MYCN*-nonamplified *MYC*-expressing SK-N-AS cells (Fig. 2c-e). Consistent with a known role of RUVBL1/2 multiprotein complex in regulating the maturation and stability of phosphatidylinositol 3-kinase-related kinase (PIKK) family of proteins, including ATM and ATR,[27,34,59] downregulation of RUVBL1/2 in NB cells also led to reduction in ATR and ATM protein levels (Fig. 2f-g). The latter are key regulators of the DDR and maintenance of genome integrity in eukaryotic cells.[60] As expected, knockdown resulted in increased DNA damage in SK-N-AS, evidenced by induction of γH2AX, a *bonafide* marker of double-strand DNA breaks, and increased apoptosis, demonstrated by immunoblotting through induction of cleaved PARP and cleaved caspase 3 in both NB1 and SK-N-AS (Fig. 2f-g).

RUVBL1/2 ATPase inhibitor, CB-6644, induces DNA damage response and suppresses growth of high-risk NB cell lines.

To further investigate RUVBL1/2 as potential therapeutic target in high-risk NB, we treated seven different NB cell lines, with diverse genetic backgrounds, with a recently reported small molecule inhibitor, CB-6644,

which specifically blocks the ATPase activity of RUVBL1/2 complex.[33] We determined the average inhibitory concentration (IC_{50}) to assess the sensitivity of CB-6644. Resazurin assay for cell viability showed that NB cell lines were inhibited by CB-6644 in the nano- to micromolar range (Figure S3a). We selected two *MYCN*-amplified cell lines, CLB-BA and NB1, and two *MYCN*-nonamplified cell lines, CLB-GA, and SK-N-AS, to further evaluate the effect of CB-6644. Both short-term (5 days) and long-term (14 days) treatment with CB-6644 led to complete block of NB cell proliferation (Fig. 3a-e).

Biochemical analyses showed that CB-6644 treatment, like the siRNA knockdown, caused reduction of ATM expression in a time-dependent manner, in four independent NB cell lines (Fig. 3f). Interestingly, ATR total protein showed a moderate decrease at 24 and 48 hrs post CB-6644 treatment and a more robust decrease at 72 hrs. In contrast, pChk1^{S345}, a marker of replication stress, increased during the earlier time periods (Fig. 3f). The increased Chk1 phosphorylation was reversed by the ATR inhibitor elimusertib (BAY-1895344) (Figure S3b), suggesting the involvement of ATR in the transient hyperphosphorylation of Chk1 upon RUVBL1/2 inhibition (Fig. 3f). At 72 hrs after CB-6644 treatment, pChk1^{S345} phosphorylation levels decreased, coinciding with a significant increase in the expression of the DNA damage marker, γH2AX, and induction of apoptosis as evidenced by elevated expression of cleaved PARP and cleaved caspase 3 (Fig. 3f). To examine the effect of CB-6644 on cell cycle, NB cells were treated with the inhibitor for 48 hrs, leading to S-phase arrest (Fig. 3g-h), consistent with other previously reported findings.[34]

Altogether, these results suggest that inhibition of RUVBL1/2 elicits a DNA damage/replication stress response and induction of S-*phase* arrest. The sustained replication stress ultimately culminates in a robust DNA damage and apoptosis, at later time points, in NB cell lines.

RUVBL1/2 regulate *MYCN* expression in NB cells.

Aberrant expression of *MYC(N)* drives subsets of high-risk NB tumours,[18,61] however, pharmacological approaches to directly target these MYC TFs have largely been unsuccessful. We showed that either siRNA-mediated knockdown or pharmacological inhibition of RUVBL1/2 led to remarkable reduction in the protein levels of N-Myc and C-Myc in NB cell lines (Fig. 2f-g, Fig. 3f). Quantitative PCR (qPCR) analysis of CB-6644 treated cells revealed that RUVBL1/2 transcriptionally regulate *MYCN* and *MYC* as evidenced by reduction in their mRNA levels in *MYCN*-amplified CLB-BA and high *MYC*-expressing SK-N-AS cells, respectively (Fig. 4a-b). This result is consistent with recent findings which showed that RUVBL1/2 mediate Pol II clustering, a mechanism of transcriptional regulation of genes, including *MYC*.[26] RNA Pol II clusters are transcriptional factories consisting of multiple RNA Pol II enzymes. They form at active transcription sites, like promoters or enhancers, and play a vital role in coordination and enhancement of gene expression and genome organization.[26,62,63] This suggests that RUVBL1/2 regulate expression of the MYC family TFs in NB cells. Conversely, previous transcriptomics and chromatin immunoprecipitation sequencing (ChIP-seq) analyses have also identified *RUVBL1/2* as direct transcriptional targets of both N-Myc and C-Myc in NB cell lines.[61] To confirm these findings in our cell lines, we induced N-Myc expression in SH-EP^{MYCN} cells. Doxycycline-induced N-Myc expression resulted

in moderate upregulation of RUVBL1 and RUVBL2 protein levels in the cells (Fig. 4c). All together, these results suggest RUVBL1/2 and N-Myc may regulate each other in NB cell lines.

To gain further insight into the importance of *RUVBL1/2* expression in *MYCN*-driven tumorigenesis, we treated NB cells derived from freshly dissociated *Th-MYCN* mice tumours of variable genotypes *(Alk-F1178S*KI/0;*Th-MYCN*Tg/0 *and Th-MYCN*Tg/0),[50,51] with increasing concentrations of CB-6644 for 5 days. Treatment with the drug potently reduced cancer cell viability in a dose-dependent manner (Fig. 4d), thereby reinforcing *RUVBL1/2* as dependency genes in NB pathogenesis.

RUVBL1/2 inhibition initiates transcriptional responses in NB cells.

To investigate the downstream transcriptional response to *RUVBL1/2* inhibition, we performed RNA-seq of *MYCN*-amplified CLB-BA and *MYCN*-nonamplified, *MYC* expressing SK-N-AS cell lines, after treatment with 250 nM CB-6644 for 24, 48 and 72 hrs. CLB-BA cells treated for 72 hrs showed the strongest differential gene expression, with a downregulation of 656 genes and an upregulation of 980 genes (Log2 fold change threshold of +/-1 at 1% FDR) (Fig. 5a). The transcriptional response increased progressively over time with 250 (15.3%), 1039 (63.3%) and 1636 (100%) genes being differentially expressed at 24, 48 and 72 hrs, respectively. A similar trend was observed in SK-N-AS cells (Figure S4a-f, Table S2 and S3).

A Hallmark gene set enrichment analysis (GSEA) indicated a significant depletion in CLB-BA cells for *MYC* signature (*Padj =* 2.4e-48), E2F transcription factors (*Padj* = 6.7e-27), G2/M checkpoints (1.1e-20) and mTORC1 signalling (*Padj =* 1.0e-22) (Fig. 5a-b, Table S4). The depletion for mTORC1 gene set is consistent with the role of RUVBL1/2 complex, together with heat shock protein 90 (HSP90), in acting as chaperone for the assembly and stability of protein complexes including mTOR.[64] On the other hand, significant enrichment was found for the p53 (*Padj =* 9.6e-9) and apoptosis pathways (*Padj =* 1.0e-4) (Fig. 5a-b). An additional GSEA using gene sets derived from Reactome largely corroborated these findings. It additionally revealed depletion of S-phase (*Padj =* 1.03e-11) and DDR pathway activities, including ATR response to replication stress (*Padj* = 2.02e-3) and double-strand break repair (*Padj =* 8.47e-5) (Figure S4g, Table S5), which agreed with our results shown above (Fig. 3f-h). Strikingly, nonsense-mediated mRNA decay (NMD) (*Padj =* 1.25e-16) was among the topmost enriched pathways, and extension of telomeres (*Padj =* 1.70e-4) and telomere maintenance (*Padj* = 3.31e-2) pathways, which are frequently activated in high-risk NB tumours,[9] were also enriched (Figure S4g). This is consistent with the roles of RUVBL1/2 complex in regulating *TERT* (*telomerase reverse transcriptase)* expression (Fig. 5a) and NMD,[30,59,65] suggesting a conservation of RUVBL1/2 function in NB and specificity of the RUVBL1/2 inhibitor, CB-6644 (Figure S4g). Genes correlated with *RUVBL1/2* expression in human primary NB tumours showed a remarkable similarity in pathway enrichment to CB-6644 treated NB cell lines (Figure S5a-b, Table S6, Fig. 5b). This further strengthens the indication of CB-6644's specificity in targeting RUVBL1/2. Additionally, a TF prediction analysis revealed that MYC and E2F family members play significant roles in mediating RUVBL1/2 transcriptional signalling. Other predicted TFs included p53, SOX11, and RUVBL1 itself, which is the target of CB-6644 (Fig. 5c).

Notably, after 72 hrs of CB-6644 treatment, *RRM2* (*ribonucleotide reductase subunit M2*), a crucial gene for DNA replication and repair, was identified among the top 20 significantly differentially expressed genes in our dataset (Fig. 5a). Our previous study revealed increased *RRM2* mRNA levels in NB tumours due to chromosome 2p gains or high-level amplification of *RRM2* copy number.[66] RRM2 functions downstream of the ATR-Chk1 replication stress response pathway, and its enforced expression alleviated replication stress in high-risk NB cells.[66] Furthermore, we demonstrated complete tumour regression in ALK-driven NB mouse models through ATR inhibition.[67] In this study, significant enrichment for ATR and RRM2 target genes upon RUVBL1/2 inhibition was observed (Figure S6a-b). Building upon these findings, we further investigated the impact of combined RUVBL1/2 and ATR inhibition on NB cell growth.

Combined RUVBL1/2 and ATR inhibition synergistically induces apoptosis in NB cells.

Our results suggest that inhibition of RUVBL1/2 activity affects ATR signalling and decrease NB cells tolerance to replication stress, exposing a therapeutic vulnerability. Therefore, we explored a therapeutic strategy of combinatorial treatment of cells with CB-6644 and the ATR inhibitor elimusertib. CB-6644 and elimusertib synergistically inhibited growth of NB1 and SH-SY5Y cell lines with combination indices (CI) of 0.80 and 0.89 respectively (Fig. 6a-b). This drug combination showed additive effect in SK-N-AS cell line (Fig. 6c). Biochemically, the combination treatment, in three independent high-risk NB cell lines, potently induced expression of γH2AX, cleavage of caspases 3 and PARP, compared to negligible to moderate induction and cleavage of same proteins in the single drug-treated cells (CB-6644 or elimusertib) (Fig. 6d-f). These showed that the combination treatment potently induced DNA damage and apoptosis in NB cell lines.

Discussion

MYC TFs are one of the most potent oncogenes in high-risk NB. However, their lack of apparent surfaces for small molecule binding makes them difficult to target directly for therapeutic purposes.[18,23] In this study, we identified *RUVBL2* as a key interactor of the *MYC* gene. *RUVBL2* forms a protein complex with *RUVBL1* and together they regulate the transcriptional activities of C-Myc and β-catenin.[36,68,69] RUVBL1/2 protein complexes have been implicated in various biological processes, including DDR, chromatin remodelling, and telomerase assembly.[28,30,31,59,64,70] These processes play critical roles in cancer development, and the oncogenic functions of RUVBL1/2 have been suggested in different cancer types.[34–36]

The RUVBL1/2 complex is involved in the control of the activity and stability of PIKK family members, such as ATM, ATR, and DNA-PKcs, which are important regulators of the circuitry coordinating the cellular DDR and replication stress.[59,64] In this study, inhibiting RUVBL1/2 activity led to decreased levels of total ATM protein (as early as 24 hrs) and phosphorylated ATR (most noticeable after 24 hrs) in NB cell lines, indicating a conserved role of RUVBL1/2 in NB cells. Consequently, RUVBL1/2 inhibition caused S-phase arrest, DNA damage and triggered apoptosis. These findings align with previous reports highlighting the anti-cancer effects of small chemical molecules targeting the RUVBL1/2 complex in other cancer cell

types.[33–35] Our results suggest that NB cells treated with the RUVBL1/2 inhibitor, CB-6644, experienced an exacerbation of replication stress or DDR activity, which was made obvious by hyperphosphorylation of Chk1^{S345} within 24 to 48 hrs post treatment with CB-6644. This ATR-Chk1 response was not sustained, possibly due to the progressive decline in both phosphorylated ATR^{S428} and Chk1 protein levels and collapsed after 72 hrs with concomitant induction of DNA damage and apoptosis. This suggests that compromising RUVBL1/2 function in NB could negatively impact replication stress response and DDR, causing checkpoint problems which may result in cell death. This scenario is supported by recent study,[69] which demonstrated that RUVBL1/2 depletion induces replication stress, specifically caused by replication-transcription conflicts, leading to compromised genome integrity during S-phase. Considering that cancer cells frequently experience replication stress,[71] it is plausible that RUVBL1/2 functions as a dependency factor in this context. In this study, we highlighted the RUVBL1/2-ATR-Chk1 signalling axis and demonstrated that the combined inhibition of RUVBL1/2 and ATR led to increased DNA damage and apoptosis, potentially due to enhanced replication stress. These findings serve as proof-of-concept for the promising potential of combinatorial therapeutic targeting of RUVBL1/2 along with other molecular targets in NB.

Recently, Solvie *et al*. uncovered a novel function of C-Myc, whereby C-Myc multimers accumulate near stalled replication forks, safeguarding them against Pol II-mediated replication stress and reducing double-strand break formation.[72] The decrease in N-Myc or C-Myc levels triggered by CB-6644 indicates a potential role of this effect in exacerbating replication stress or DDR activity in NB cells. It is intriguing to note that RUVBL1/2, along with other factors, is required for C-Myc multimer formation,[72] underscoring the intricate connection between RUVBL1/2 and MYC(N) in the regulation of replication stress in cells.

RUVBL1/2 functions as a cofactor by interacting with Pol II in chromatin, facilitating Pol II clustering and transcription initiation.[26] Interestingly, formation of Pol II clusters is dependent on RUVBL1/2's ATPase activity,[26] which can be inhibited by CB-6644.[33] We showed that inhibition of RUVBL1/2 with CB-6644 in NB cells initiated transcriptional response, including significant depletion in *MYCN* or *MYC* levels. This could be attributed to a possible decrease in Pol II clusters, which could affect expression of RUVBL1/2-Pol II axis target genes including *MYC*.[26] Our transcriptomic analysis also highlighted MYC(N) and E2F targets as the top two significantly depleted gene sets in NB cells treated with CB-6644. This depletion in MYC(N) targets may be due to decrease in N-MYC or C-Myc transcriptional activity resulting from the reduction in its mRNA and protein levels. Additionally, C-Myc plays a key role in transcriptional pause release of Pol II - a central regulatory mechanism controlling over 70% of genes.[73] RUVBL1/2 interacts with C-Myc,[74,75] to facilitate C-Myc-dependent transcriptional pause release of Pol II leading to increase transcriptional activity.[69] It is plausible that inhibition of RUVBL1/2 may affect this interaction leading to decrease in gene expression. E2F1 also is known to recruit RUVBL1/2, in ATPase domain-dependent manner, to open the chromatin conformation at E2F target genes, thereby amplifying the E2F transcriptional response.[76,77] Hence inhibition of RUVBL1/2 ATPase activity with CB-6644 could interfere

with this recruitment, resulting in downregulation of E2F target genes. In brief, MYC and E2F family TFs may act as effectors for RUVBL1/2 downstream signalling in high-risk NB.

In our cell line models, we observed a significant delay in cell growth or apoptotic response after inhibiting RUVBL1/2. This delay could be attributed to the delayed transcriptional response observed following the inhibition, which may be influenced by the role of RUVBL1/2 as coactivators. Coactivators typically exhibit slower transcriptional responses compared to transcriptional activators known for their ability to elicit faster transcriptional responses.

In summary, we propose that in NB cells, RUVBL1/2 positively regulate stability and activity of ATR and expression of *MYCN* or *MYC* to modulate replication stress and promote cell survival and proliferation (Fig. 7).[26,59,64,72] Hence inhibition of RUVBL1/2 aggravates replication stress, which in-turn activates the ATR-Chk1 response pathway to deal with this stress. Sustained ATR-Chk1 replication stress response and Myc multimer shielding of replication folks are dependent on ATR activity and protein stability and MYC(N) levels respectively. Therefore, simultaneous inhibition of RUVBL1/2 in this scenario leads to decline in MYC(N) expression and ATR activity, and a concomitant collapse of the stress response, leading to DNA damage and apoptosis (Fig. 7).

This study highlighted the multipronged roles of RUVBL1/2 in regulating the key oncogenic pathways, including MYC(N) signalling and ATR-Chk1 replication stress response in high-risk NB, and demonstrated *RUVBL1/2* as independent prognostic biomarkers in NB. In conclusion, our study unveils the putative clinical utility of *RUVBL1/2* in high-risk NB both as a biomarker and as exploitable therapeutic targets, thus strongly motivates their further exploration for clinical translation in NB.

Declarations

Conflicts of interests

All authors declare no competing interests.

Availability of Data and Materials

RNA-seq data are available in ArrayExpress (https://www.ebi.ac.uk/arrayexpress/, accession number E-MTAB-13137). Data are interactively available using the CLEAN web application with https://ccgg.ugent.be/shiny/clean/siaw_2023/. All other data required to evaluate the conclusions in the paper are provided in Supplementary information files. Source data are provided with this paper.

Code availability

Source code used for RNA-Seq and public data analyses is available at GitHub https://github.com/CCGGlab/RUVBL.

Contributors

This study was conceptualized and designed by JTS, RHP and JVdE. For investigation: qPCR analyses and cell viability assays of mouse NB cells were performed by W-YL and MB, cell cycle experiments were conducted by EH and supervised by FS and KD, JTS conducted all other wet-lab experimental analyses, and JTS, AC and JVdE performed the bioinformatic analyses. JTS, BH, RHP and JVdE drafted the manuscript, with subsequent review and editing from all authors.

Acknowledgements

This project was funded by grants from the Swedish Childhood Cancer Foundation (TJ2021-0068 - JTS; PR2022-0029 - RHP; PR2021-27 - BH), the Assar Gabrielsson's foundation (FB22-24 - JTS), the Ghent University Special Research Fund (BOF.STG.2019.0073.01 - JVdE; BOF.GOA.2022.0003.03 - FS), Kom op tegen Kanker (Stand up to Cancer), the Flemish cancer society (STI.VLK.2022.0013.01 -AC), the Swedish Cancer Society (CAN21/1459 - RHP; CAN21/1525 - BH), Villa Joep grant (FS) and the Research Foundation Flanders (FWO; FWO.OPR.2023.0063.01 - FS, JVdE, RHP).

References

1. Kameneva P, Artemov AV, Kastriti ME, Faure L, Olsen TK, Otte J, et al. Single-cell transcriptomics of human embryos identifies multiple sympathoblast lineages with potential implications for neuroblastoma origin. Nature genetics. 2021;53(5):694-706.
2. Jansky S, Sharma AK, Körber V, Quintero A, Toprak UH, Wecht EM, et al. Single-cell transcriptomic analyses provide insights into the developmental origins of neuroblastoma. Nature genetics. 2021;53(5):683-93.
3. Ladenstein R, Pötschger U, Pearson ADJ, Brock P, Luksch R, Castel V, et al. Busulfan and melphalan versus carboplatin, etoposide, and melphalan as high-dose chemotherapy for high-risk neuroblastoma (HR-NBL1/SIOPEN): an international, randomised, multi-arm, open-label, phase 3 trial. The Lancet Oncology. 2017;18(4):500-14.
4. Park JR, Kreissman SG, London WB, Naranjo A, Cohn SL, Hogarty MD, et al. Effect of Tandem Autologous Stem Cell Transplant vs Single Transplant on Event-Free Survival in Patients With High-Risk Neuroblastoma: A Randomized Clinical Trial. Jama. 2019;322(8):746-55.
5. Cohn SL, Pearson AD, London WB, Monclair T, Ambros PF, Brodeur GM, et al. The International Neuroblastoma Risk Group (INRG) classification system: an INRG Task Force report. Journal of clinical oncology : official journal of the American Society of Clinical Oncology. 2009;27(2):289-97.
6. Suh E, Stratton KL, Leisenring WM, Nathan PC, Ford JS, Freyer DR, et al. Late mortality and chronic health conditions in long-term survivors of early-adolescent and young adult cancers: a retrospective cohort analysis from the Childhood Cancer Survivor Study. The Lancet Oncology. 2020;21(3):421-35.
7. Irwin MS, Naranjo A, Zhang FF, Cohn SL, London WB, Gastier-Foster JM, et al. Revised Neuroblastoma Risk Classification System: A Report From the Children's Oncology Group. Journal of clinical oncology : official journal of the American Society of Clinical Oncology. 2021;39(29):3229-41.

8. London WB. WANTED: Better neuroblastoma biomarkers and better stratification. EBioMedicine. 2022;86:104358.
9. Ackermann S, Cartolano M, Hero B, Welte A, Kahlert Y, Roderwieser A, et al. A mechanistic classification of clinical phenotypes in neuroblastoma. Science (New York, NY). 2018;362(6419):1165-70.
10. Peifer M, Hertwig F, Roels F, Dreidax D, Gartlgruber M, Menon R, et al. Telomerase activation by genomic rearrangements in high-risk neuroblastoma. Nature. 2015;526(7575):700-4.
11. Cheung NK, Zhang J, Lu C, Parker M, Bahrami A, Tickoo SK, et al. Association of age at diagnosis and genetic mutations in patients with neuroblastoma. Jama. 2012;307(10):1062-71.
12. Carén H, Kryh H, Nethander M, Sjöberg RM, Träger C, Nilsson S, et al. High-risk neuroblastoma tumors with 11q-deletion display a poor prognostic, chromosome instability phenotype with later onset. Proceedings of the National Academy of Sciences of the United States of America. 2010;107(9):4323-8.
13. Janoueix-Lerosey I, Schleiermacher G, Michels E, Mosseri V, Ribeiro A, Lequin D, et al. Overall genomic pattern is a predictor of outcome in neuroblastoma. Journal of clinical oncology : official journal of the American Society of Clinical Oncology. 2009;27(7):1026-33.
14. Lopez G, Conkrite KL, Doepner M, Rathi KS, Modi A, Vaksman Z, et al. Somatic structural variation targets neurodevelopmental genes and identifies SHANK2 as a tumor suppressor in neuroblastoma. Genome research. 2020;30(9):1228-42.
15. Siaw JT, Javanmardi N, Van den Eynden J, Lind DE, Fransson S, Martinez-Monleon A, et al. 11q Deletion or ALK Activity Curbs DLG2 Expression to Maintain an Undifferentiated State in Neuroblastoma. Cell reports. 2020;32(12):108171.
16. Otte J, Dyberg C, Pepich A, Johnsen JI. MYCN Function in Neuroblastoma Development. Frontiers in oncology. 2020;10:624079.
17. Singh S, Quarni W, Goralski M, Wan S, Jin H, Van de Velde LA, et al. Targeting the spliceosome through RBM39 degradation results in exceptional responses in high-risk neuroblastoma models. Science advances. 2021;7(47):eabj5405.
18. Zimmerman MW, Liu Y, He S, Durbin AD, Abraham BJ, Easton J, et al. MYC Drives a Subset of High-Risk Pediatric Neuroblastomas and Is Activated through Mechanisms Including Enhancer Hijacking and Focal Enhancer Amplification. Cancer discovery. 2018;8(3):320-35.
19. Wang LL, Teshiba R, Ikegaki N, Tang XX, Naranjo A, London WB, et al. Augmented expression of MYC and/or MYCN protein defines highly aggressive MYC-driven neuroblastoma: a Children's Oncology Group study. British journal of cancer. 2015;113(1):57-63.
20. Huang M, Weiss WA. Neuroblastoma and MYCN. Cold Spring Harb Perspect Med. 2013;3(10):a014415.
21. Soucek L, Jucker R, Panacchia L, Ricordy R, Tatò F, Nasi S. Omomyc, a potential Myc dominant negative, enhances Myc-induced apoptosis. Cancer research. 2002;62(12):3507-10.

22. Beaulieu ME, Martínez-Martín S, Kaur J, Castillo Cano V, Massó-Vallés D, Foradada Felip L, et al. Pharmacokinetic Analysis of Omomyc Shows Lasting Structural Integrity and Long Terminal Half-Life in Tumor Tissue. Cancers. 2023;15(3).
23. Puissant A, Frumm SM, Alexe G, Bassil CF, Qi J, Chanthery YH, et al. Targeting MYCN in neuroblastoma by BET bromodomain inhibition. Cancer discovery. 2013;3(3):308-23.
24. Otto T, Horn S, Brockmann M, Eilers U, Schüttrumpf L, Popov N, et al. Stabilization of N-Myc is a critical function of Aurora A in human neuroblastoma. Cancer cell. 2009;15(1):67-78.
25. Gu L, Zhang H, He J, Li J, Huang M, Zhou M. MDM2 regulates MYCN mRNA stabilization and translation in human neuroblastoma cells. Oncogene. 2012;31(11):1342-53.
26. Wang H, Li B, Zuo L, Wang B, Yan Y, Tian K, et al. The transcriptional coactivator RUVBL2 regulates Pol II clustering with diverse transcription factors. Nature communications. 2022;13(1):5703.
27. Dauden MI, López-Perrote A, Llorca O. RUVBL1-RUVBL2 AAA-ATPase: a versatile scaffold for multiple complexes and functions. Curr Opin Struct Biol. 2021;67:78-85.
28. Poli J, Gerhold CB, Tosi A, Hustedt N, Seeber A, Sack R, et al. Mec1, INO80, and the PAF1 complex cooperate to limit transcription replication conflicts through RNAPII removal during replication stress. Genes & development. 2016;30(3):337-54.
29. Vassileva I, Yanakieva I, Peycheva M, Gospodinov A, Anachkova B. The mammalian INO80 chromatin remodeling complex is required for replication stress recovery. Nucleic Acids Res. 2014;42(14):9074-86.
30. Venteicher AS, Meng Z, Mason PJ, Veenstra TD, Artandi SE. Identification of ATPases pontin and reptin as telomerase components essential for holoenzyme assembly. Cell. 2008;132(6):945-57.
31. Jónsson ZO, Dhar SK, Narlikar GJ, Auty R, Wagle N, Pellman D, et al. Rvb1p and Rvb2p are essential components of a chromatin remodeling complex that regulates transcription of over 5% of yeast genes. The Journal of biological chemistry. 2001;276(19):16279-88.
32. Rodríguez CF, Llorca O. RPAP3 C-Terminal Domain: A Conserved Domain for the Assembly of R2TP Co-Chaperone Complexes. Cells. 2020;9(5).
33. Assimon VA, Tang Y, Vargas JD, Lee GJ, Wu ZY, Lou K, et al. CB-6644 Is a Selective Inhibitor of the RUVBL1/2 Complex with Anticancer Activity. ACS Chem Biol. 2019;14(2):236-44.
34. Yenerall P, Das AK, Wang S, Kollipara RK, Li LS, Villalobos P, et al. RUVBL1/RUVBL2 ATPase Activity Drives PAQosome Maturation, DNA Replication and Radioresistance in Lung Cancer. Cell Chem Biol. 2020;27(1):105-21.e14.
35. Shin SH, Lee JS, Zhang JM, Choi S, Boskovic ZV, Zhao R, et al. Synthetic lethality by targeting the RUVBL1/2-TTT complex in mTORC1-hyperactive cancer cells. Science advances. 2020;6(31):eaay9131.
36. Wood MA, McMahon SB, Cole MD. An ATPase/helicase complex is an essential cofactor for oncogenic transformation by c-Myc. Mol Cell. 2000;5(2):321-30.

37. Pugh TJ, Morozova O, Attiyeh EF, Asgharzadeh S, Wei JS, Auclair D, et al. The genetic landscape of high-risk neuroblastoma. Nature genetics. 2013;45(3):279-84.
38. A comprehensive assessment of RNA-seq accuracy, reproducibility and information content by the Sequencing Quality Control Consortium. Nat Biotechnol. 2014;32(9):903-14.
39. Wang C, Gong B, Bushel PR, Thierry-Mieg J, Thierry-Mieg D, Xu J, et al. The concordance between RNA-seq and microarray data depends on chemical treatment and transcript abundance. Nat Biotechnol. 2014;32(9):926-32.
40. Cangelosi D, Morini M, Zanardi N, Sementa AR, Muselli M, Conte M, et al. Hypoxia Predicts Poor Prognosis in Neuroblastoma Patients and Associates with Biological Mechanisms Involved in Telomerase Activation and Tumor Microenvironment Reprogramming. Cancers. 2020;12(9).
41. De Wyn J, Zimmerman MW, Weichert-Leahey N, Nunes C, Cheung BB, Abraham BJ, et al. MEIS2 Is an Adrenergic Core Regulatory Transcription Factor Involved in Early Initiation of TH-MYCN-Driven Neuroblastoma Formation. Cancers. 2021;13(19).
42. Phipson B, Lee S, Majewski IJ, Alexander WS, Smyth GK. ROBUST HYPERPARAMETER ESTIMATION PROTECTS AGAINST HYPERVARIABLE GENES AND IMPROVES POWER TO DETECT DIFFERENTIAL EXPRESSION. Ann Appl Stat. 2016;10(2):946-63.
43. Dempster JM, Rossen J, Kazachkova M, Pan J, Kugener G, Root DE, et al. Extracting Biological Insights from the Project Achilles Genome-Scale CRISPR Screens in Cancer Cell Lines. bioRxiv. 2019:720243.
44. Foroutan M, Bhuva DD, Lyu R, Horan K, Cursons J, Davis MJ. Single sample scoring of molecular phenotypes. BMC Bioinformatics. 2018;19(1):404.
45. Liberzon A, Birger C, Thorvaldsdóttir H, Ghandi M, Mesirov JP, Tamayo P. The Molecular Signatures Database (MSigDB) hallmark gene set collection. Cell Syst. 2015;1(6):417-25.
46. Shannon P, Markiel A, Ozier O, Baliga NS, Wang JT, Ramage D, et al. Cytoscape: a software environment for integrated models of biomolecular interaction networks. Genome research. 2003;13(11):2498-504.
47. Therneau TM. A Package for Survival Analysis in R. 2023.
48. Korotkevich G, Sukhov V, Budin N, Shpak B, Artyomov M, Sergushichev A. Fast gene set enrichment analysis. bioRxiv; 2016.
49. Wu T, Hu E, Xu S, Chen M, Guo P, Dai Z, et al. clusterProfiler 4.0: A universal enrichment tool for interpreting omics data. Innovation (Camb). 2021;2(3):100141.
50. Borenäs M, Umapathy G, Lai WY, Lind DE, Witek B, Guan J, et al. ALK ligand ALKAL2 potentiates MYCN-driven neuroblastoma in the absence of ALK mutation. The EMBO journal. 2021;40(3):e105784.
51. Weiss WA, Aldape K, Mohapatra G, Feuerstein BG, Bishop JM. Targeted expression of MYCN causes neuroblastoma in transgenic mice. The EMBO journal. 1997;16(11):2985-95.

52. Chou TC. Theoretical basis, experimental design, and computerized simulation of synergism and antagonism in drug combination studies. Pharmacol Rev. 2006;58(3):621-81.
53. Kim D, Langmead B, Salzberg SL. HISAT: a fast spliced aligner with low memory requirements. Nature methods. 2015;12(4):357-60.
54. Anders S, Pyl PT, Huber W. HTSeq–a Python framework to work with high-throughput sequencing data. Bioinformatics. 2015;31(2):166-9.
55. Love MI, Huber W, Anders S. Moderated estimation of fold change and dispersion for RNA-seq data with DESeq2. Genome Biol. 2014;15(12):550.
56. Cloutier P, Poitras C, Durand M, Hekmat O, Fiola-Masson É, Bouchard A, et al. R2TP/Prefoldin-like component RUVBL1/RUVBL2 directly interacts with ZNHIT2 to regulate assembly of U5 small nuclear ribonucleoprotein. Nature communications. 2017;8:15615.
57. Serna M, González-Corpas A, Cabezudo S, López-Perrote A, Degliesposti G, Zarzuela E, et al. CryoEM of RUVBL1-RUVBL2-ZNHIT2, a complex that interacts with pre-mRNA-processing-splicing factor 8. Nucleic Acids Res. 2022;50(2):1128-46.
58. Haurie V, Ménard L, Nicou A, Touriol C, Metzler P, Fernandez J, et al. Adenosine triphosphatase pontin is overexpressed in hepatocellular carcinoma and coregulated with reptin through a new posttranslational mechanism. Hepatology. 2009;50(6):1871-83.
59. Izumi N, Yamashita A, Iwamatsu A, Kurata R, Nakamura H, Saari B, et al. AAA+ proteins RUVBL1 and RUVBL2 coordinate PIKK activity and function in nonsense-mediated mRNA decay. Science signaling. 2010;3(116):ra27.
60. Awasthi P, Foiani M, Kumar A. ATM and ATR signaling at a glance. J Cell Sci. 2015;128(23):4255-62.
61. Westermann F, Muth D, Benner A, Bauer T, Henrich KO, Oberthuer A, et al. Distinct transcriptional MYCN/c-MYC activities are associated with spontaneous regression or malignant progression in neuroblastomas. Genome Biol. 2008;9(10):R150.
62. Iborra FJ, Pombo A, Jackson DA, Cook PR. Active RNA polymerases are localized within discrete transcription "factories' in human nuclei. J Cell Sci. 1996;109 (Pt 6):1427-36.
63. Wansink DG, Schul W, van der Kraan I, van Steensel B, van Driel R, de Jong L. Fluorescent labeling of nascent RNA reveals transcription by RNA polymerase II in domains scattered throughout the nucleus. The Journal of cell biology. 1993;122(2):283-93.
64. Izumi N, Yamashita A, Ohno S. Integrated regulation of PIKK-mediated stress responses by AAA+ proteins RUVBL1 and RUVBL2. Nucleus. 2012;3(1):29-43.
65. Li W, Zeng J, Li Q, Zhao L, Liu T, Björkholm M, et al. Reptin is required for the transcription of telomerase reverse transcriptase and over-expressed in gastric cancer. Molecular cancer. 2010;9:132.
66. Nunes C, Depestel L, Mus L, Keller KM, Delhaye L, Louwagie A, et al. RRM2 enhances MYCN-driven neuroblastoma formation and acts as a synergistic target with CHK1 inhibition. Science advances. 2022;8(28):eabn1382.

67. Szydzik J, Lind DE, Arefin B, Kurhe Y, Umapathy G, Siaw JT, et al. ATR inhibition enables complete tumour regression in ALK-driven NB mouse models. Nature communications. 2021;12(1):6813.
68. Feng Y, Lee N, Fearon ER. TIP49 regulates beta-catenin-mediated neoplastic transformation and T-cell factor target gene induction via effects on chromatin remodeling. Cancer research. 2003;63(24):8726-34.
69. Hristova RH, Stoynov SS, Tsaneva IR, Gospodinov AG. Deregulated levels of RUVBL1 induce transcription-dependent replication stress. Int J Biochem Cell Biol. 2020;128:105839.
70. Mao YQ, Houry WA. The Role of Pontin and Reptin in Cellular Physiology and Cancer Etiology. Front Mol Biosci. 2017;4:58.
71. da Costa A, Chowdhury D, Shapiro GI, D'Andrea AD, Konstantinopoulos PA. Targeting replication stress in cancer therapy. Nat Rev Drug Discov. 2023;22(1):38-58.
72. Solvie D, Baluapuri A, Uhl L, Fleischhauer D, Endres T, Papadopoulos D, et al. MYC multimers shield stalled replication forks from RNA polymerase. Nature. 2022;612(7938):148-55.
73. Rahl PB, Young RA. MYC and transcription elongation. Cold Spring Harb Perspect Med. 2014;4(1):a020990.
74. Koch HB, Zhang R, Verdoodt B, Bailey A, Zhang CD, Yates JR, 3rd, et al. Large-scale identification of c-MYC-associated proteins using a combined TAP/MudPIT approach. Cell cycle (Georgetown, Tex). 2007;6(2):205-17.
75. Bellosta P, Hulf T, Balla Diop S, Usseglio F, Pradel J, Aragnol D, et al. Myc interacts genetically with Tip48/Reptin and Tip49/Pontin to control growth and proliferation during Drosophila development. Proceedings of the National Academy of Sciences of the United States of America. 2005;102(33):11799-804.
76. Tarangelo A, Lo N, Teng R, Kim E, Le L, Watson D, et al. Recruitment of Pontin/Reptin by E2f1 amplifies E2f transcriptional response during cancer progression. Nature communications. 2015;6:10028.
77. Wang R, Li X, Sun C, Yu L, Hua D, Shi C, et al. The ATPase Pontin is a key cell cycle regulator by amplifying E2F1 transcription response in glioma. Cell death & disease. 2021;12(2):141.

Figures

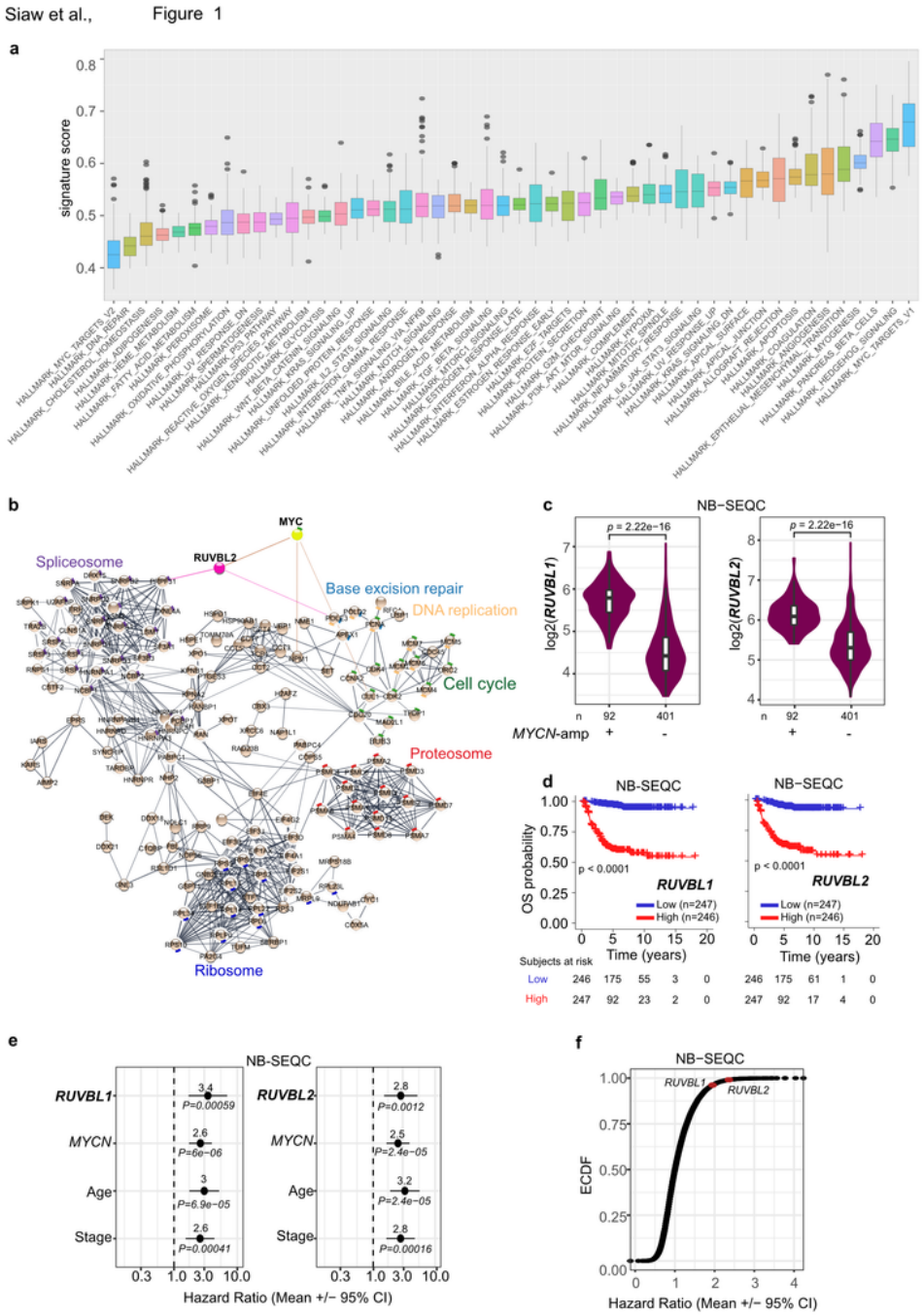

Figure 1

***MYC* signature and network analyses of high-risk NB tumours**. (**a**) Box plots represent Hallmark gene set signature scores in high-risk NB tumours (NB-TARGET; n=129). (**b**) STRING network analysis of *MYC targets v1* gene set. Functional modules indicated in the network. (**c**) Violin plots showing *RUVBL1* and RUVBL*2* mRNA levels in *MYCN*-amplified and non-amplified tumours as indicated. Data derived from in NB-SEQC cohorts of primary NB tumours. (**d-f**) Overall survival (OS) analysis using publicly available data

from the NB-SEQC cohort (n=498). High/low *RUVBL*1/2 expression defined based on the median expression value. (**d**) Kaplan-Meier survival plots showing association of *RUVBL1* and *RUVBL2* mRNA levels (high/low) with OS probability. (**e**) Cox proportional hazards multivariate regression analysis using 4 variables as indicated. Forest plots showing hazard ratios (HRs) +/- 95% confidence intervals. (**f**) Empirical cumulative distribution function (ECDF) plot showing multivariate HRs calculated for all 19,667 coding genes. Source data are provided as a Source Data file.

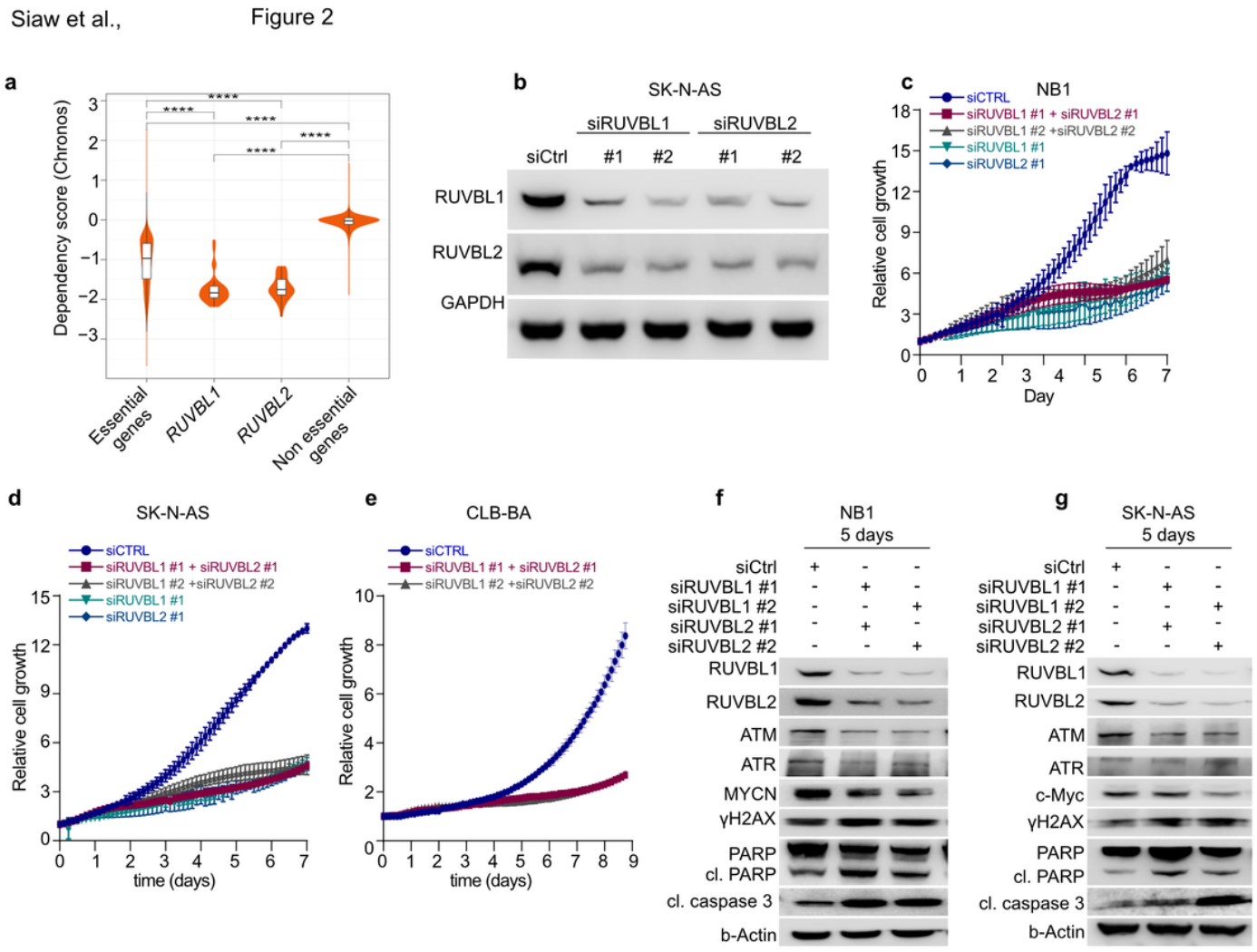

Figure 2

Effect of siRNA-mediated knockdown of *RUVBL1/2* in NB cell lines. (**a**) Violin plots comparing DepMap *RUVBL1* and *RUVBL2* dependency scores from 34 NB cell lines to sets of essential and non-essential genes. ****, *P*<0.0001, unpaired Wilcox test. (**b**) Western blot showing transient siRNA-mediated knockdown of RUVBL1 and RUVBL2 after 3 days of transfection. Scrambled siRNA was used as control (siCtrl). (**c-e**) Time-courses showing the effect of knockdown of *RUVBL1* and/or *RUVBL2* on cell proliferation in three NB cell lines, as indicated. Cell proliferation was monitored live by scanning for cell confluency at regular time intervals with IncuCyte® S3 system. Each time point represents the mean +/-

SEM of least three independent experiments. (**f-g**) Western blot showing the effect of RUBL1/2 knockdown on downstream signalling molecules in NB cell lines after 5 days of transfection for 2 NB cell lines as indicated. cl denotes cleaved. Blots are representative of at least two independent experiments.

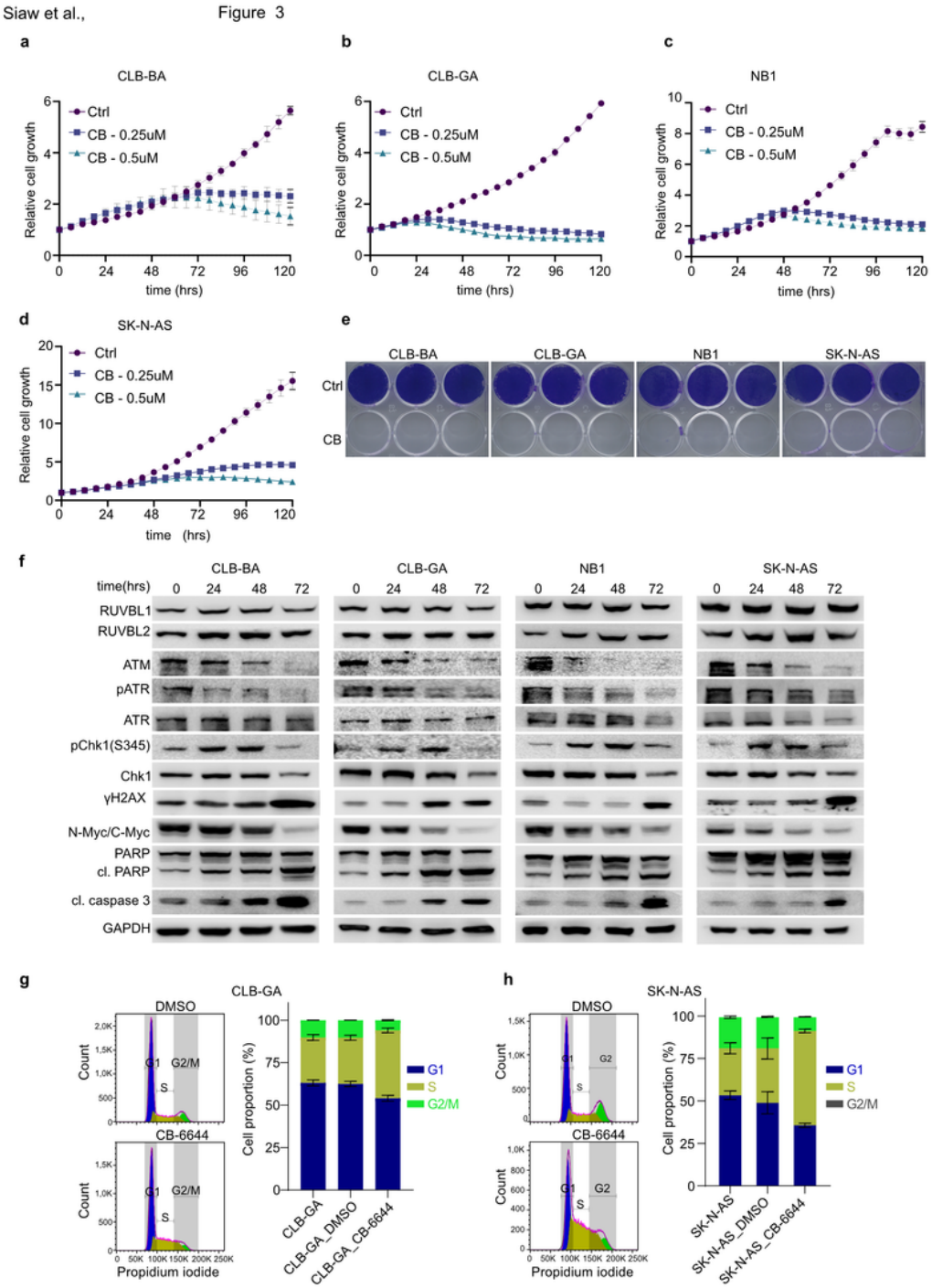

Figure 3

Pharmacological inhibition of RUVBL1/2 ATPase activity with CB-6644, in NB cell lines. (**a-d**) Time-dependent effect of the RUVBL1/2 inhibitor CB-6644 (250 nM or 500 nM as indicated) on proliferation of NB cell lines. Cell growth was monitored by scanning cell confluency at regular intervals with IncuCyte® Live Cell Analysis system. Cell growth is normalized relative to the first scan at time zero. Results are mean +/- SEM of 3 independent biological replicates. (**e**) Long-term (14 days) effect of CB-6644 (250 nM) on NB cell growth. Cells were stained with crystal violet. (**f**) Western blot analyses showing the effect of CB-6644 (250 nM) on downstream signalling of RUVBL1/2. N-Myc/C-Myc denotes N-Myc for CLB-BA, CLB-GA and NB1, and C-Myc for SK-N-AS which were detected by two independent antibodies. cl denotes cleaved. Blots are representative of at least 2 independent experiments. (**g-h**) Flow cytometry-based cell cycle analyses of propidium iodide-stained NB cell lines treated for 48 hrs with DMSO or CB-6644 at IC50 concentrations for (**g**) CLB-GA (120 nM) and (**h**) SK-N-AS (250 nM). Stacked bar charts show cell proportions in each cycle phase, at different conditions, for two experimental repeats.

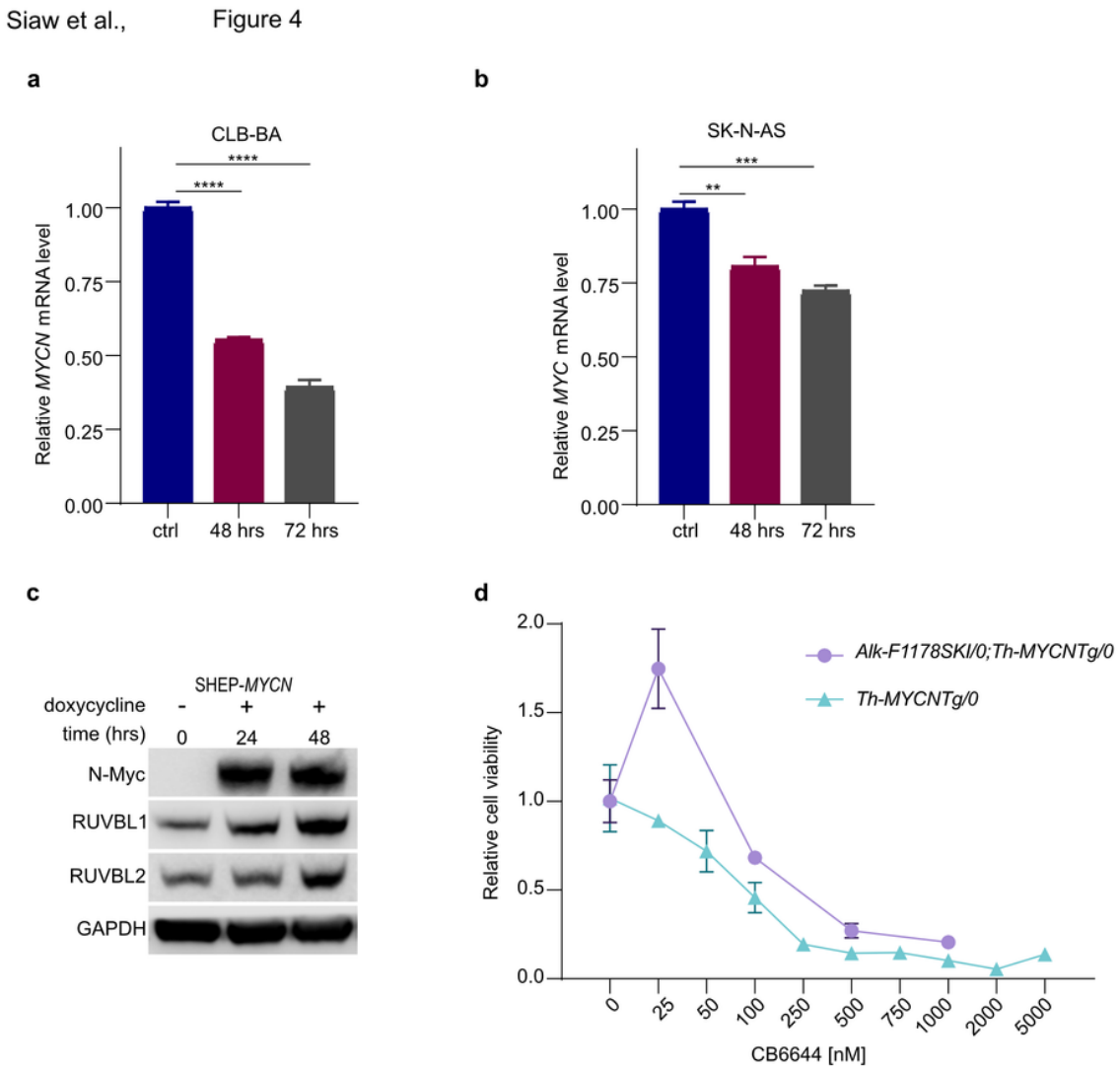

Figure 4

Role of RUVBL1/2 in regulation of *MYCN* expression. Bar plots showing time-dependent effects of RUVBL1/2 inhibition with CB-6655 (250 nM) on (**a**), *MYCN* mRNA (in CLB-BAR, *MYCN*-amplified cell line) and (**b**) *MYC* (in SK-N-AS, MYCN-nonamplified cell line) as determined by quantitative PCR. Results are means +/- SEM of three independent biological replicates. (**c**) Western blot showing effect of doxycycline inducible *MYCN* overexpression in SHEP cells on RUVBL1 and RUVBL2 protein expression. (**d**) Graph showing the effect of increasing concentration of CB-6644 on viability of mice NB cells derived from freshly dissociated tumours. Cell viability was measured after 5 days. Cells were derived from tumours of variable genetic background as indicated.

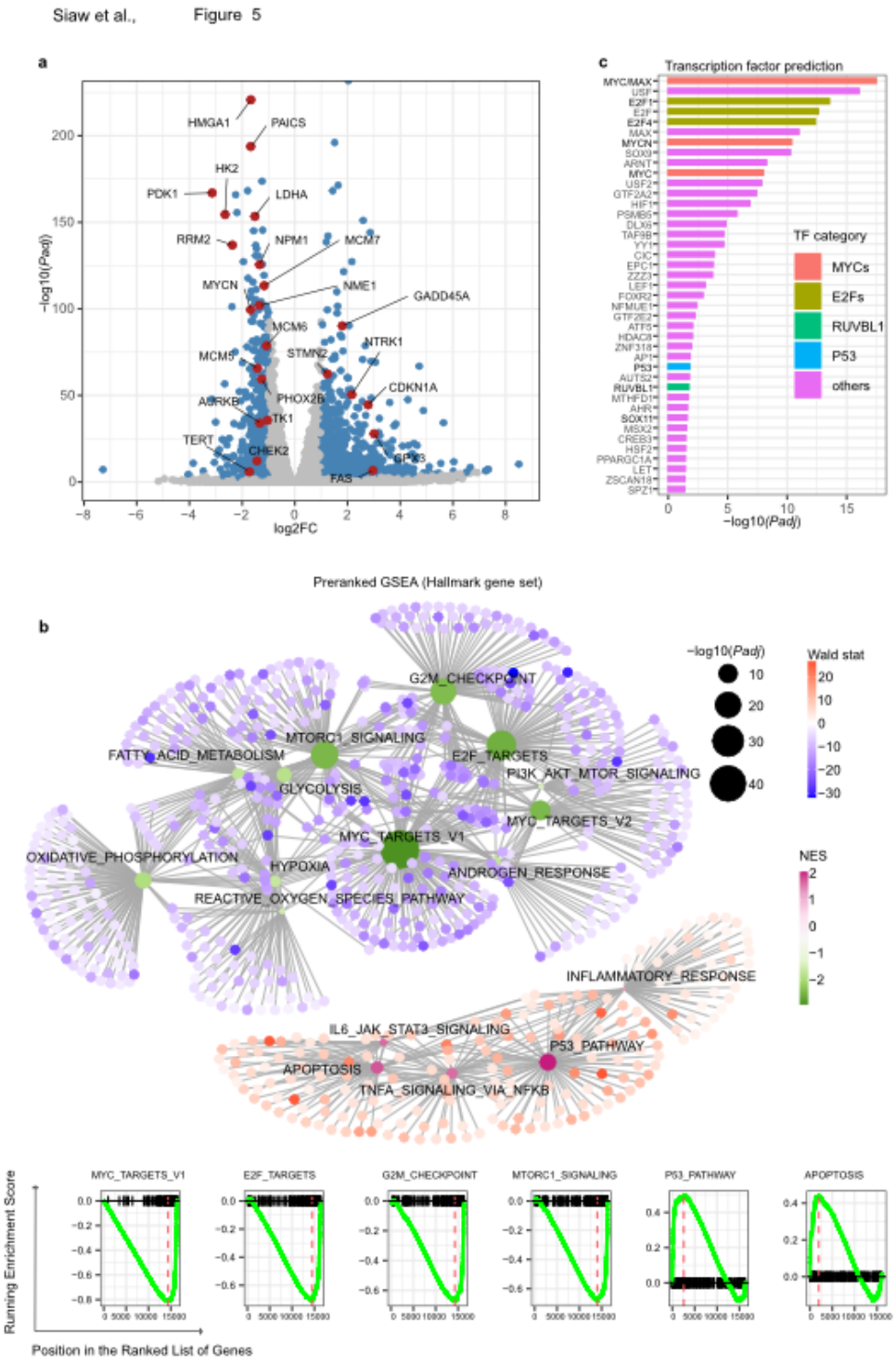

Figure 5

Transcriptomic response to CB-6644 treatment of NB cells. (**a**) Volcano plot showing the transcriptomic response to RUVBL1/2 inhibition with CB-6644 (250 nM) for 72 hrs in CLB-BA. Differentially expressed genes (DEGs; log2FoldChange ±1 at 1% FDR) are indicated in blue, whereas genes labelled and indicated in red are examples of key DEGs. (**b**) Network graph showing Hallmark GSEA results (CLB-BA response 72 hrs). The sizes of central nodes denote -log10 adjusted *P* values of gene sets which are coloured based

on their normalized enrichment scores (NES). Nodes radiating from a central node (gene set) denote genes belonging to that gene set, and genes are coloured based on their DESseq2 Wald stat as indicated in legend. Bottom panels represent running score plots for key significantly enriched gene sets as indicated. (**c**) Bar plot showing results of transcription factor prediction by GSEA based on transcription factor target gene set. Bars represent adjusted *P* values (−log10 scale) for enriched transcription factors at 5% FDR. Key transcription factor categories are coloured as indicated in legend. Source data are provided as a Source Data file.

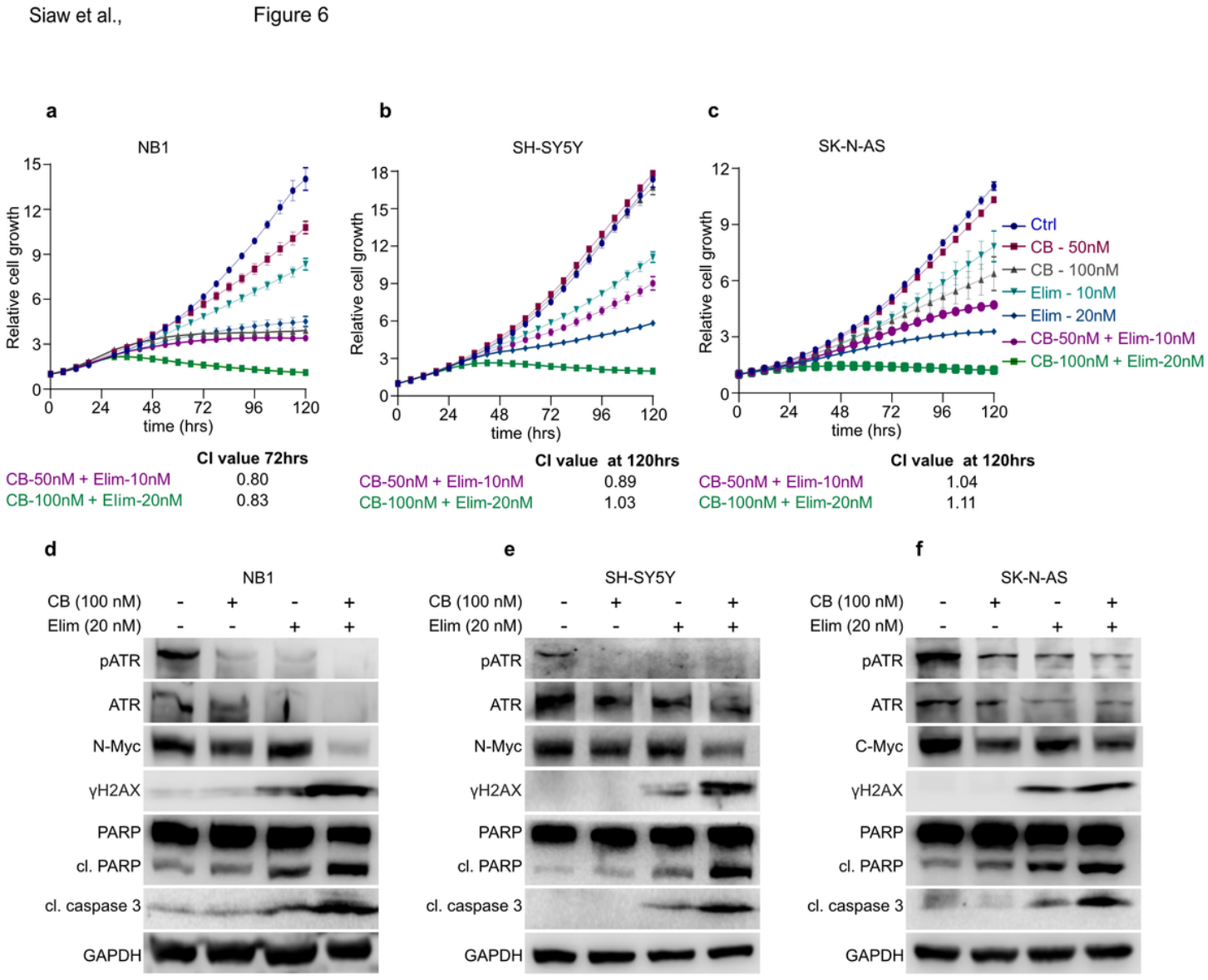

Figure 6

Effect of combined RUVBL1/2 and ATR inhibition NB cell growth. (**a-c**) Time-courses showing the effect of CB-6644 (CB, RUVBL1/2 inhibitor) or elimusertib (Elim, ATR inhibitor) alone or in combination on NB cell proliferation. Cell growth was monitored by scanning cell confluency at regular intervals with

IncuCyte® Live Cell Analysis system. Cell growth is normalized relative to the first scan at time zero. Results are mean +/- SEM of 2 independent biological replicates. Synergy between CB-6644 and elimusertib was calculated with CompuSyn software and values expressed as combination index (CI). (**d-f**) Western blot showing the effect of CB-6644 +/- elimusertib on DNA damage (γH2AX) and apoptotic markers (cleaved (cl) caspase 3, PARP) in NB cells. Cells were treated with inhibitors for 48 hrs.

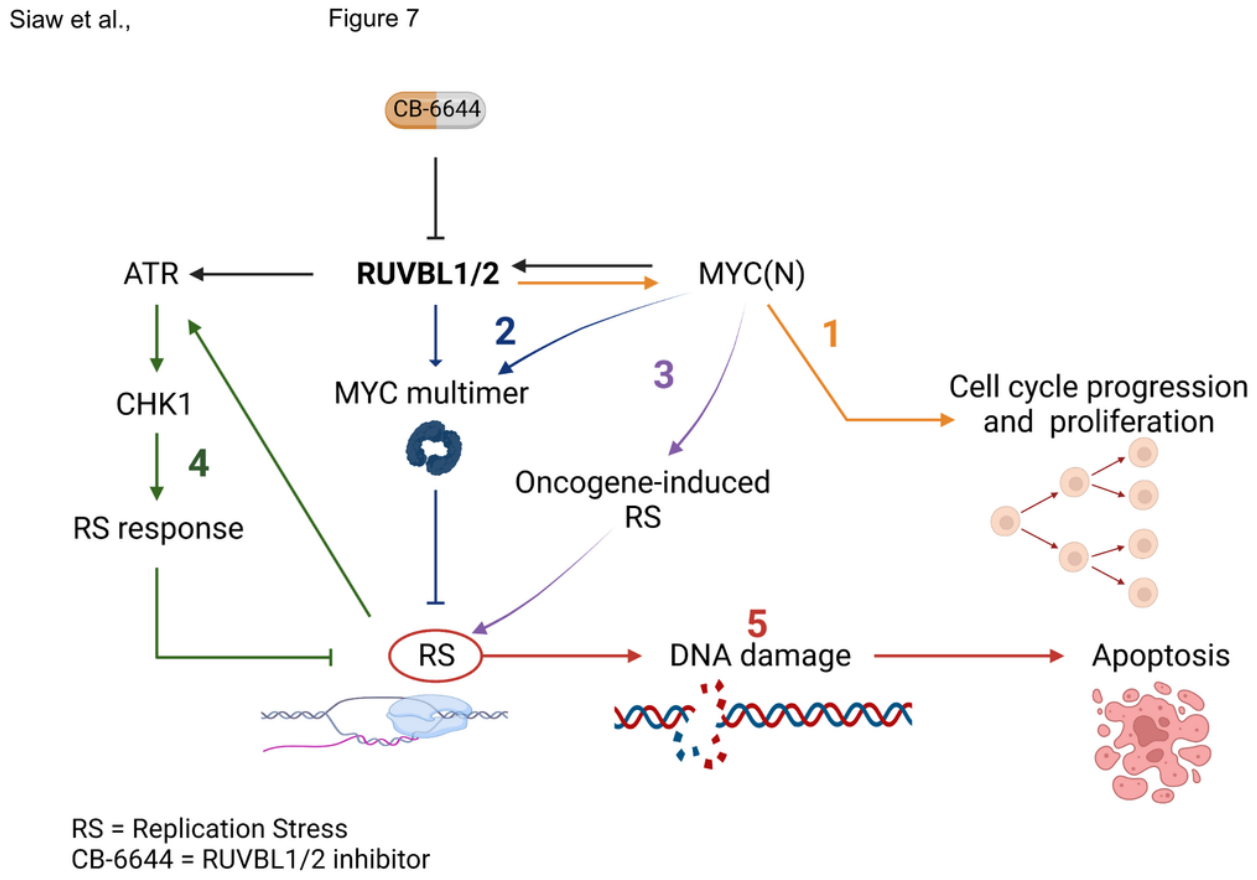

Figure 7

Schematic summary. (1; orange axis) RUVBL1/2 positively regulate *MYCN* or *MYC* expression to promote cell cycle progression, proliferation and (2; blue axis) formation of MYC multimers which guard against replication stress (RS).[72] (3; purple axis) Activation of oncogenic proteins, including MYC(N) induces RS in cancer cells due to transcription-replication conflicts.[69] Inhibition of RUVBL1/2 exacerbates RS, which in-turn (4; green axis) activates the ATR-Chk1 response pathway to deal with this stress. RUVBL1/2 positively regulates ATR protein stability and *MYC(N)* expression, thereby sustaining ATR-Chk1 and MYC multimer RS signalling response. Therefore, inhibition of RUVBL1/2 in this scenario leads to gradual decline in ATR activity and MYC multimer levels, leading to concurrent collapse of the RS stress or DNA damage response, resulting in (5; red axis) DNA damage and apoptosis. Figure was created with Biorender.com.

Supplementary Files

This is a list of supplementary files associated with this preprint. Click to download.

- TableS1rescoxphallgenesSeqcAndCangelosi.xlsx
- TableS2resDESEq2sknasba.xlsx
- TableS3numDEgenessknasba.xlsx
- TableS4resgseaHBA72h.xlsx
- TableS5resgseaREACTOMEBA72h.xlsx
- TableS6resgseaHtumour.xlsx
- SupFigure1.tif
- SupFigure2.tif
- SupFigure3.tif
- SupFigure4.tif
- SupFigure5.tif
- SupFigure6.tif